Protective effect of H$_2$S on LPS-induced AKI by promoting autophagy

TING LI[1*], JIE ZHAO[2*], SHUYING MIAO[3], YIYANG CHEN[3], YUNFEI XU[3] and YING LIU[3]

[1]Department of Physiology, Changzhi Medical College, Changzhi, Shanxi 046000;
[2]Department of Neurosurgery, Xiangya Hospital; [3]Department of Pathophysiology,
Xiangya School of Medicine, Central South University, Changsha, Hunan 410078, P.R. China

Abstract. The present study explored the protective effect of exogenous hydrogen sulfide (H$_2$S) on lipopolysaccharide (LPS)-induced acute kidney injury (AKI) and the underlying mechanisms. To establish an AKI injury mouse model, LPS (10 mg/kg) was intraperitoneally injected into mice pretreated with 0.8 mg/kg sodium hydrosulfide hydrate (NaHS), an H$_2$S donor. The mouse survival rate and the degree of kidney injury were examined. To construct a cell damage model, HK-2 cells were pretreated with different concentrations (0.1, 0.3 and 0.5 mM) of NaHS, and then the cells were stimulated with LPS (1 μg/ml). The cell viability, autophagy, apoptosis levels and the release of inflammatory factors were examined in mouse kidney tissue and HK-2 renal tubular epithelial cells. It was found that pretreatment with NaHS significantly improved the survival rate of septic AKI mice, and reduced the renal damage, release of inflammatory factors and apoptosis. In HK-2 cells, NaHS protected cells from LPS caused damage via promoting autophagy and inhibiting apoptosis and the release of inflammatory factors. In order to clarify the relationship between autophagy and apoptosis and inflammatory factors, this study used 3-methyladenine (3-MA) to inhibit autophagy. The results revealed that 3-MA eliminated the protective effect of NaHS in HK-2 cells and AKI mice. Overall, NaHS can protect from LPS-induced AKI by promoting autophagy and inhibiting apoptosis and the release of inflammatory factors.

Introduction

Sepsis is one of the serious complications of critically ill patients with trauma, shock, infection and major surgery. It is a primary cause of septic shock and multiple organ dysfunction syndrome (MODS) (1,2). The mortality rate of sepsis remains high, and sepsis with acute kidney injury (AKI) is an independent risk factor for the poor prognosis of critically ill patients (3-5). Currently, AKI has become a major problem in critical care medicine. Although early diagnosis and renal replacement therapy continues to improve, the mortality rate of patients with AKI caused by sepsis remains high, posing a huge threat to human health and social economy (6). Therefore, finding new methods for the treatment of septic AKI will help to establish novel treatment strategies and reduce the high incidence and fatality rate of septic AKI.

Hydrogen sulfide (H$_2$S) is the third gas signal molecule discovered after nitric oxide (NO) and carbon monoxide (CO), and has a wide range of biological functions in the body. H$_2$S shows important pathophysiological significance for the occurrence and development of various diseases, and has great potential in therapeutic application (7). An increased number of studies have shown that low concentrations of H$_2$S may have a protective effect against AKI caused by factors such as sepsis. For example, sodium hydrosulfide hydrate (NaHS) treatment on rats can reduce cisplatin-induced nephrotoxicity (8). NaHS can reduce renal ischemia-reperfusion injury through anti-oxidation, anti-inflammatory and anti-apoptotic effects (9-11). H$_2$S can play a protective role in diabetic nephropathy through a variety of mechanisms (12-14). NaHS can also prevent the renal function damage caused by ureteral obstruction (15-17), and H$_2$S reduces LPS-induced AKI damage through anti-inflammatory and antioxidant effects (18). Albeit these findings, the mechanism of the protective effect of H$_2$S on AKI has not been fully elucidated.

Autophagy is ubiquitous in most eukaryotic cells. It is a self-protection phenomenon that involves the formation of autophagosomes, which are double-layer membrane structures that wrap the damaged organelles, denatured proteins and various macromolecular substances; the

Correspondence to: Professor Ting Li, Department of Physiology, Changzhi Medical College, 161 Jiefang East Street, Changzhi, Shanxi 046000, P.R. China
E-mail: sllit@czmc.edu.cn

Professor Ying Liu, Department of Pathophysiology, Xiangya School of Medicine, Central South University, 87 Xiangya Road, Changsha, Hunan 410078, P.R. China
E-mail: liu1977ying@126.com

*Contributed equally

autophagosomes are transported to lysosomes to form autophagolysosomes that degrades the contents, thereby maintaining cell survival, renewal, material reuse and internal environment stability (19,20). A number of studies have shown that autophagy has a protective effect on AKI models (21-25). Therefore, proper induction of autophagy might be able to improve the prognosis of AKI caused by sepsis. Studies have shown that H$_2$S can promote autophagy levels (26,27), however, the relationship between autophagy and apoptosis or inflammatory factors in LPS-induced AKI has not yet been reported. In order to make up for this shortcoming, the present study was performed.

In this study, the LPS-induced mouse AKI model and HK-2 renal tubular epithelial cell injury model were used to explore the effects of exogenous H$_2$S on LPS-induced AKI. Immunofluorescence, western blotting and other methods were used to examine the effect of H$_2$S on LPS-induced kidney cell injury. Autophagy inhibitor was used to investigate whether the protective effect of H$_2$S was through regulating autophagy.

Materials and methods

Animals. A total of 140 male C57BL/6 mice (8 weeks old) were purchased from Hunan SJA Laboratory Animal Co., Ltd., with an average weight of 20-25 g. Mice were fed in a clean and quiet environment at a temperature of 25°C and humidity of 40-60% and allowed free access to food and water. Mice were kept at 12/12 h light and dark cycles. To observe the effect of NaHS on the survival rate of LPS-induced AKI mice, 60 mice were randomly divided into three groups (n=20): i) Control group; ii) LPS group; and iii) LPS + NaHS (0.8 mg/kg) group. The mice in the LPS intervention groups were intraperitoneally injected with LPS (10 mg/kg; Sigma-Aldrich; Merck KGaA), and the control group was injected with the same amount of saline. The NaHS intervention group was intraperitoneally injected with NaHS (Sigma-Aldrich; Merck KGaA) 30 min before LPS injection, and the survival was observed every 12 h until the 72-h point. To investigate the effect of NaHS on LPS-induced kidney damage, 40 mice were randomly divided into four groups (n=10): i) Control group; ii) NaHS group; iii) LPS group; and iv) LPS + NaHS group. Mice in the LPS + NaHS group were injected with NaHS (0.8 mg/kg) 30 min before LPS injection. Then, 12 h later, blood was collected from the mice, and the mice were sacrificed to collect kidney tissue. To investigate the effect of 3-MA on the protective effect of NaHS, 40 mice were randomly divided into four groups (n=10): i) Control group; ii) LPS group; iii) LPS + NaHS group; and iv) LPS + NaHS + 3-MA group. Previous studies have shown that 3-MA (30 mg/kg) injected intraperitoneally for 30 min before NaHS or other drugs can effectively inhibit the level of autophagy (28,29). Therefore, in the LPS + NaHS + 3-MA group, 3-MA (30 mg/kg) was injected intraperitoneally at first; 30 min later, NaHS (0.8 mg/kg) was injected, followed by LPS injection at 30 min later. Then, 12 h later, mice were anesthetized through isoflurane (2%) inhalation and blood was collected, and then mice were euthanized by cervical dislocation to collect kidney tissues. All animal experiments were approved by the Institutional Animal Ethics Committee of Central South University (approval no. 2021101119; Changsha, China). Both our preliminary experiments and

literature reports showed that 3-MA alone did not increase damage, therefore our experiment did not set up a 3-MA group alone (30).

Renal function test. After blood collection, the blood was allowed to stand at room temperature for 2 h, centrifuged at 1,000 x g for 15 min at 4°C, and the serum was collected. An automatic biochemical analyzer (Hitachi, Ltd.) was used to detect renal function indicators, such as blood urea nitrogen (BUN) and creatinine levels.

Hematoxylin and eosin (H&E) staining. Fresh mouse kidney tissue was fixed in 4% paraformaldehyde solution for 24 h at room temperature, embedded in paraffin and sectioned at 4-μm thickness. H&E staining was performed to observe the tissue damage condition. The sample was incubated with hematoxylin for ~3-5 min at room temperature. After washing, the sample was incubated with eosin for ~2 min at room temperature. Kidney morphology was observed under an optical microscope. Blind method (investigator-blinded) was used to score the degree of injury: i) 0 points, normal; ii) 1 point, renal tubular injury area <25%; iii) 2 points, 25~50%; iv) 3 points, 50~75%; and v) 4 points, 75~100%.

Transmission electron microscopy. After collection, the fresh kidney tissue was completely fixed in the 2.5% glutaraldehyde solution at 4°C for 2-4 h. Then, the tissues were sent to Wuhan Servicebio Technology Co., Ltd., to prepare the specimens. Briefly, kidney tissue was post-fixed in 1% osmium tetroxide, dehydrated in a graded series of ethanol (50-100%) and acetone, embedded in Epon and sectioned at 60-80 nm, and then images were collected under a transmission electron microscope.

Terminal deoxynucleotidyl-transferase-mediated dUTP nick end labeling (TUNEL) assay. The fresh kidney tissue was fixed in 4% paraformaldehyde solution for 24 h at room temperature, embedded in paraffin and sectioned at 4-μm thickness. TUNEL apoptosis detection kit (cat. no. 1684817910; Sigma-Aldrich; Merck KGaA) was used to detect the level of apoptosis in paraffin-embedded sections of kidney tissue. The specific procedures followed the manufacturer's instructions. The sections were then incubated with DAB (cat. no. DM827; Dako; Agilent Technologies, Inc.). When the cell nucleus was brown under the light microscope, the section was washed to stop the staining. Then, Harris hematoxylin was used to counterstain the nucleus for 3 min at room temperature. Images were observed under light microscopy (magnification, x200). Positive cells were counted at x200 magnification. The percentage of apoptosis was calculated as the number of apoptotic cells/total number of cells x100% in 5-10 randomly selected fields.

Enzyme-linked immunosorbent assay (ELISA). ELISA kit was used to detect the levels of interleukin (IL)-6 (cat. no. EK0411), tumor necrosis factor-α (TNF-α; cat. no. EK0527), IL-1β (cat. no. EK0394; Wuhan Boster Biological Technology, Ltd.) and IL-18 (cat. no. CSB-E04609m; Cusabio Technology LLC) in mouse kidney tissue. The specific procedures followed the kit instructions.

Cell culture. The HK-2 cell line was purchased from American Type Culture Collection and maintained in DMEM/F12 medium (Gibco; Thermo Fisher Scientific, Inc.) supplemented with 10% fetal bovine serum (Gibco; Thermo Fisher Scientific, Inc.) at 37°C and 5% CO_2. The medium was renewed every 2-3 days. The HK-2 cells were plated in a 6-well plate at $1x10^5$ cells/well and divided into four groups: i) Control; ii) NaHS; iii) LPS; and iv) LPS + NaHS group. The cells in the LPS + NaHS group were pre-incubated with 0.1 mM NaHS for 30 min and then stimulated with 1,000 ng/ml LPS for 12 h at 37°C and 5% CO_2. Following which, the cells were collected for further analysis. For the 3-MA experiment, the HK-2 cells were plated in a 6-well plate at $1x10^5$ cells/well and divided into four groups: i) Control; ii) LPS; iii) LPS + NaHS; and iv) LPS + NaHS + 3-MA group. The cells in the LPS + NaHS + 3-MA group were incubated with 5 mM 3-MA for 30 min, and then 0.1 mM NaHS was added and incubated for another 30 min, followed by stimulation with 1,000 ng/ml LPS for 12 h at 37°C and 5% CO_2. The cells and supernatant were collected for further analysis.

Western blotting. RIPA lysis buffer (plus phenylmethanesulfonyl fluoride) (cat. no. WB-0072; Beijing Dingguo Changsheng Biotechnology Co., Ltd.) was used to extract protein from mouse kidney tissue and cells, and the protein concentration was determined by the BCA (cat. no. BCA01; Beijing Dingguo Changsheng Biotechnology Co., Ltd.) method. Protein samples (40 µl/lane) were added with 1/4 volume of 5X SDS loading buffer and boiled at 95°C for 10 min to denature the protein. After electrophoresis by 12% gel and transfer to 0.2 µm PVDF membrane (cat. no. ISEQ00010; MilliporeSigma), the membrane was blocked by 2% BSA (cat. no. FA016; Genview) at room temperature for 1-2 h and incubated with primary antibodies at 4°C overnight. The primary antibodies were anti-LC-3B (1:1,000; cat. no. L7543; Sigma-Aldrich; Merck KGaA), anti-p62 (1:1,000; cat. no. P0067; Sigma-Aldrich; Merck KGaA) and anti-β-actin (1:2,000; cat. no. A1978; Sigma-Aldrich; Merck KGaA). After incubation with the HRP-conjugated goat anti-rabbit IgG (H+L) (1:5,000; cat. no. AS014; ABclonal Biotech Co., Ltd.) secondary antibody at room temperature for 1 h, the membrane was developed with enhanced chemiluminescence (ECL) (cat. no. GE2301; Genview). ImageJ version 1.48 (National Institutes of Health) software was used to analyze protein bands and calculate relative protein expression.

Immunofluorescence. The slices were emersed in xylene I for 15 min, xylene II for 15 min, anhydrous ethanol I for 5 min, anhydrous ethanol II for 5 min, 85% alcohol for 5 min and 75% alcohol for 5 min, and then washed with distilled water. Then, the slices were placed in a repair box filled with EDTA antigen retrieval buffer (pH 8.0) in a microwave oven for antigen retrieval. The fire was stopped for 8 min at medium heat for 8 min and switched to low fire for 7 min. After natural cooling, the slides were placed in PBS (pH 7.4) and washed three times, and then the paraffin-embedded sections (paraffin-embedded process and section thickness were the same as aforementioned) were blocked with 1% BSA (cat. no. A8020; Beijing Solarbio Science & Technology Co., Ltd.) for 30 min at 37°C, and

incubated with a primary antibody against LC-3B (1:100; cat. no. L7543; Sigma-Aldrich; Merck KGaA) overnight at 4°C. After washing with PBS, the sections were incubated with a goat anti-rabbit secondary antibody conjugated with fluorescein isothiocyanate (1:50; cat. no. AS011; ABclonal Biotech Co., Ltd.) at room temperature in the dark for 1 h. DNA was counterstained with DAPI (cat. no. C0065; Beijing Solarbio Science & Technology Co., Ltd.) for 10 min at room temperature. Images were acquired from a fluorescence microscope. For immunofluorescence staining on cells, cells were plated on a cover glass in a 6-well plate at $1x10^5$ cells/well; and then following the treatments outlined above, the cells were washed three times with PBS, fixed with 4% paraformaldehyde for 10 min at room temperature, and washed three times with PBS. The cells were blocked with 1% BSA (cat. no. A8020; Beijing Solarbio Science & Technology Co., Ltd.) for 30 min at 37°C, and the subsequent steps were the same as aforementioned for the paraffin-embedded sections.

Cell viability analysis. Cells were plated in a 96-well plate at $1x10^4$ cells/well and given the treatments outlined above. Next, the supernatant was discarded, and Cell Counting Kit-8 (CCK-8) reagent was added to detect cell viability. The specific procedures followed the instructions of the CCK-8 kit (cat. no. CK04; Dojindo Laboratories, Inc.).

Detection of lactic dehydrogenase (LDH) level in cell culture medium. The supernatant of each well in the 96-well plate was collected to detect the LDH levels. The specific procedures followed the instructions of the LDH Cytotoxicity Detection Kit (Nanjing Jiancheng Bioengineering Institute).

Detection of apoptosis via flow cytometry. The cells were trypsinized, washed and tested for apoptosis via flow cytometry (BD FACSCanto™ II flow cytometer; BD Biosciences). The detailed procedures followed the instructions of the Annexin V-FITC/PI Apoptosis Detection Kit (BD Pharmingen; BD Biosciences). Data acquisition was performed using FlowJo version 7.6.1 analysis software (FlowJo, LLC). The apoptotic rate (%) was calculated as the sum of Annexin V-FITC$^+$/PI$^-$ (early apoptosis, Q3) and Annexin-V-FITC$^+$/PI$^+$ (late apoptosis, Q2) cells.

Statistical analysis. The data were analyzed using GraphPad Prism 5 software (GraphPad Software, Inc.). All experiments were repeated at least three times. Kaplan-Meier plots were used to illustrate survival of mice between different groups, and statistical assessment was performed by the log-rank test. Bonferroni correction was used for statistical comparison between multiple groups for the analysis of survival curves ($P<0.0167$ was considered statistically significant). The median + interquartile range were used to illustrate tubular injury score of mice between different groups, and statistical assessment was performed by Kruskal-Wallis followed by Dunn's post hoc test. One-way analysis of variance (One-Way ANOVA) was used for comparison between multiple groups, followed by the Tukey's post hoc test for pairwise comparisons. $P<0.05$ was considered to indicate a statistically significant difference.
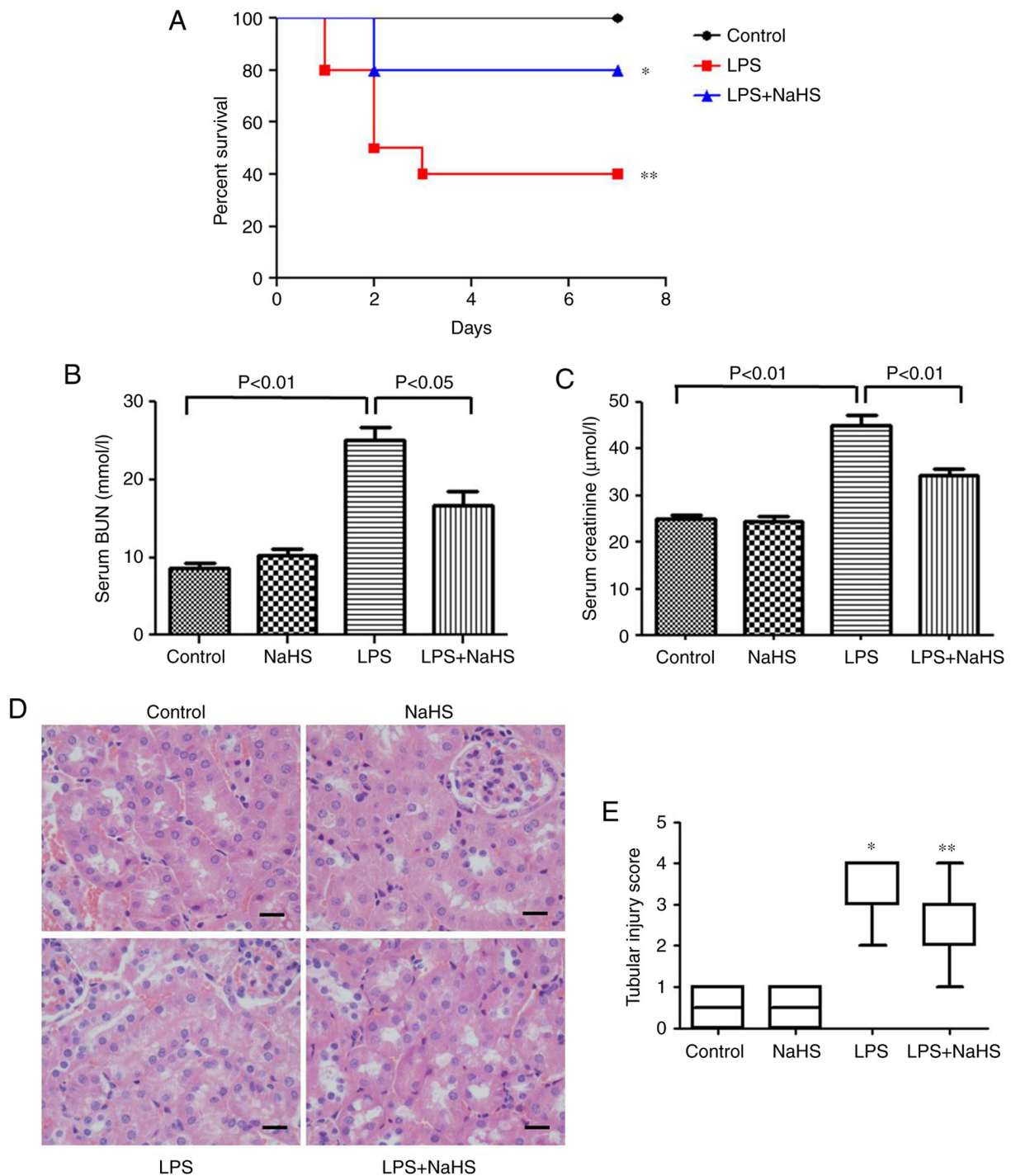
Figure 1. Hydrogen sulfide improves the survival rate of mice with LPS-induced acute kidney injury and reduces renal damage. (A) Survival curve of each group (n=20). *P<0.0167 vs. control group; **P>0.0167 vs. LPS group. (B) The serum BUN level in each group. (C) The serum creatine level of each group. (D) The morphological changes of kidney tissue in each group under light microscope (hematoxylin and eosin staining). Scale bar, 20 µm. (E) Renal histological damage score of each group. Data are presented as the mean ± SD (n=10). *P<0.01 vs. control group; **P<0.01 vs. LPS group. LPS, lipopolysaccharide; BUN, blood urea nitrogen; NaHS, sodium hydrosulfide hydrate.

Results

Effect of NaHS on the survival rate of AKI mice induced by LPS. The effect of NaHS pretreatment on the survival rate of mice injected with LPS was examined. The results showed that 0.8 mg/kg NaHS could increase the survival rate of LPS-induced mice (Fig. 1A), however, the statistical difference between the NaHS + LPS group and LPS group was not significant. This may

be related to the small sample size, and thus the sample size will be increased for further verification in subsequent experiments.

Pretreatment with NaHS reduces renal function damage and histopathological damage in mice with LPS-induced AKI. To clarify the effect of NaHS on renal function damage, BUN and creatinine levels were measured in mice injected with LPS. The results showed that LPS increased the BUN and creatinine
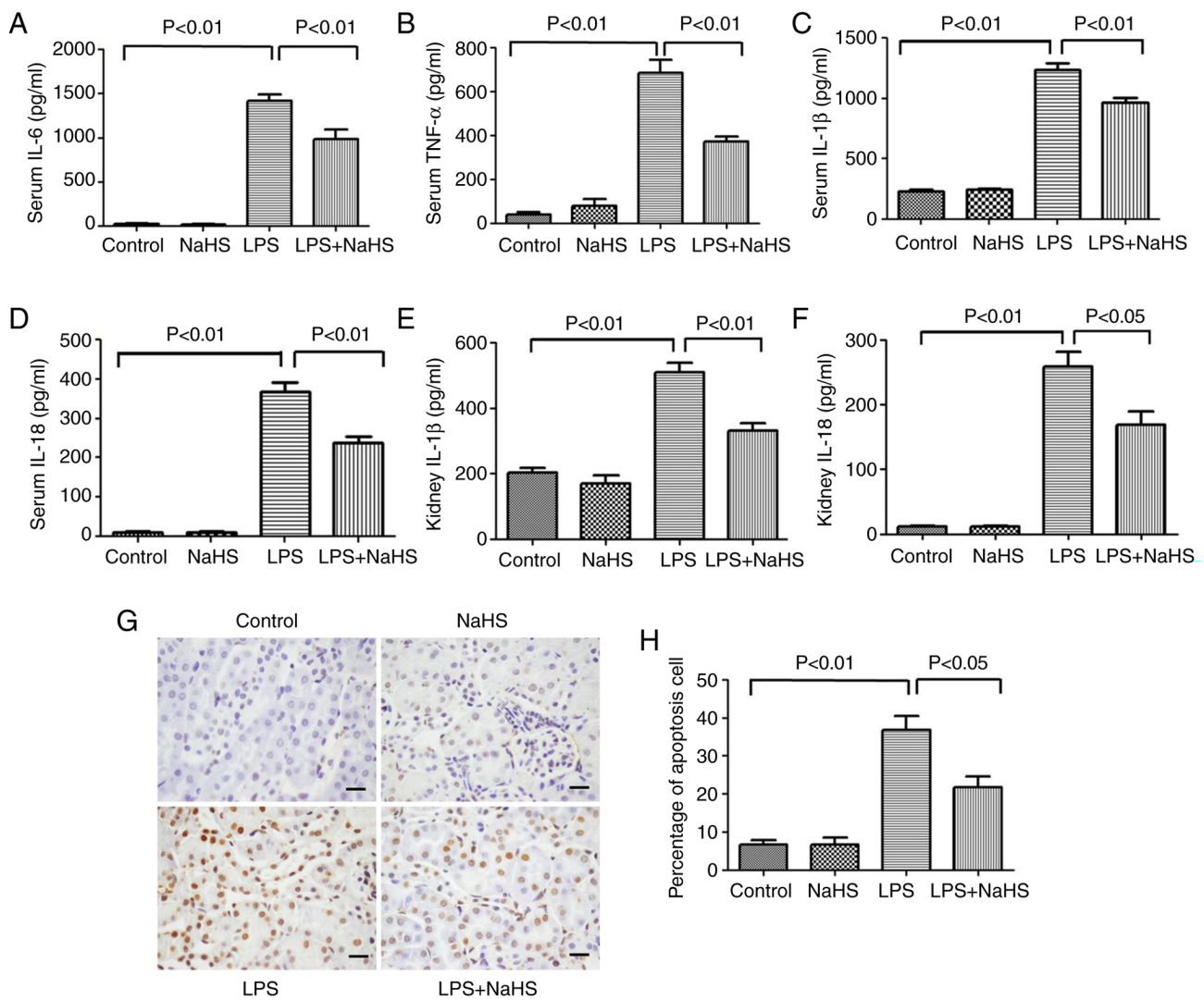
Figure 2. Hydrogen sulfide reduces the release of inflammatory factors and apoptosis in mice with LPS-induced acute kidney injury. (A) IL-6, (B) TNF-α, (C) IL-1β and (D) IL-18 levels in serum. (E) IL-1β and (F) IL-18 levels in kidney tissues. (G) TUNEL staining shows the level of apoptosis in kidney tissue. Scale bar, 20 μm. (H) Statistics of apoptosis index in kidney tissue of each group. Data are presented as the mean $\pm$ SD (n=10). LPS, lipopolysaccharide; IL, interleukin; TNF-α, tumor necrosis factor-α; NaHS, sodium hydrosulfide hydrate.

levels, which were significantly prevented by NaHS pretreatment (Fig. 1B and C). H&E staining was also performed to examine the changes in kidney morphology, and the results showed that LPS treatment caused kidney pathological changes, such as edema and granular degeneration of tubular epithelial cells, and NaHS pretreatment significantly reduced the tubular injury score induced by LPS (Fig. 1D and E).

Pretreatment with NaHS reduces inflammation in mice with LPS-induced AKI. To clarify the effect of NaHS on the release of inflammatory factors in LPS-induced mice, the expression levels of classic inflammatory factors, such as IL-6, TNF-α, IL-1β and IL-18, were measured in mouse serum after 12 h of LPS stimulation. The results showed that the serum levels of IL-6, TNF-α, IL-1β and IL-18 significantly increased after LPS treatment, while NaHS pretreatment could effectively reduce the elevation of these inflammatory factors (Fig. 2A-D). Further examination of IL-1β and IL-18 levels in kidney tissues showed that NaHS pretreatment significantly reduced the expression of IL-1β and IL-18 in kidney tissues from the

mice (Fig. 2E and F). The aforementioned results indicated that NaHS pretreatment alleviated the inflammatory response induced by LPS in both the serum and the kidney tissues.

Pretreatment with NaHS reduces the rate of apoptosis in kidney tissues of LPS-induced AKI mice. TUNEL staining was used to detect the effect of LPS on kidney cell apoptosis in AKI mice. Cell apoptosis can occur in both pathological and physiological conditions. As shown in Fig. 2G and H, very few apoptotic cells were detected in the normal control group or NaHS group. However, 12 h after LPS injection, the number of apoptotic cells with positive TUNEL staining in kidney tissues were significantly increased, and NaHS pretreatment significantly prevented the increase of apoptotic cells. These results indicated that NaHS pretreatment alleviated LPS-induced apoptosis in mouse kidney cells.

Pretreatment with NaHS reduces the LPS induced damage on HK-2 cells. To further clarify the mechanism of NaHS in LPS-induced AKI, assays at the cellular level were performed.

The HK-2 renal tubular epithelial cells were stimulated with LPS for 12 h, and the intervention groups were pretreated with different concentrations of NaHS (0.1, 0.3 and 0.5 mM). To determine the degree of cell damage, CCK-8 and LDH assays were used to detect cell viability and LDH levels in the cell culture supernatant. The results showed that LPS treatment decreased cell viability and increased the release of LDH in the supernatant, while 0.1 mM NaHS pretreatment could significantly reverse these effects. The effects of 0.3 and 0.5 mM NaHS pretreatment were not obvious (Fig. 3A and B). Therefore, 0.1 mM NaHS was chosen for pretreatment in all subsequent cell experiments.

Pretreatment with NaHS reduces the LPS-induced release of inflammatory factors and apoptosis in HK-2 cells. To clarify the effect of NaHS pretreatment on the LPS-induced release of inflammatory factors in HK-2 cells, ELISA was used to detect the release of IL-1β and IL-18 in the cell supernatant. The results showed that LPS treatment increased the release of IL-1β and IL-18 in HK-2 cells, and NaHS pretreatment significantly reduced these effects (Fig. 3C and D). Next, the present study sought to investigate the effect of NaHS pretreatment on the apoptosis of HK-2 cells induced by LPS using flow cytometry. The results showed that LPS treatment increased the fraction of apoptotic HK-2 cells, and NaHS pretreatment significantly reduced LPS-induced apoptosis (Fig. 3E and F). The aforementioned results suggested that the protective effect of NaHS on LPS-induced AKI was partially mediated by its anti-inflammatory and anti-apoptotic effects, but the underlying mechanisms are still unclear.

Pretreatment with NaHS enhances the autophagy level in HK-2 cells stimulated by LPS. To clarify the anti-inflammatory and anti-apoptotic mechanism of NaHS, the effect of NaHS on autophagy was examined. First, western blotting was performed to detect the expression of autophagy-related proteins microtubule associated protein 1 light chain 3 (LC3B) and sequestosome 1 (p62) in HK-2 cells. It was found that the expression of LC3B and p62 protein did not change when NaHS was administered alone. However, after LPS stimulation, the ratio of LC3B-II/LC3B-I increased and the expression of p62 protein decreased. NaHS pretreatment further increased the ratio of LC3B-II/LC3B-I and decreased the expression of p62 protein (Fig. 3G-I), suggesting that NaHS could promote autophagy. Immunofluorescence and electron microscopy were then used to further verify the effect of NaHS on autophagy. Immunofluorescence results showed that the punctate autophagosomes in the renal tubules increased significantly after LPS stimulation, and NaHS pretreatment further increased the number of autophagosomes (Fig. 3J and K). Electron microscopy results showed that the number of autophagic vesicles increased notably in HK-2 cells after LPS stimulation, and NaHS pretreatment further augmented this change (Fig. 3L). Altogether, these results indicated that NaHS pretreatment could enhance the autophagy level in the HK-2 cells stimulated with LPS.

Inhibition of autophagy by 3-MA reverses the protective effect of NaHS on LPS-induced HK-2 cell apoptosis and the release of inflammatory factors. Since NaHS pretreatment can further enhance the autophagy induced by LPS, the anti-inflammatory and anti-apoptotic effects of NaHS may be related to autophagy. To test this hypothesis, the autophagy inhibitor 3-MA was used to block autophagy and it was examined whether the protective effect of NaHS on HK-2 cells could be reversed. First, western blotting was used to detect the inhibitory effect of 3-MA on autophagy, and the results showed that 3-MA significantly reduced the ratio of LC3B-II/LC3B-I in the LPS + NaHS + 3-MA group, and the expression of p62 protein was increased (Fig. 4A-C). Secondly, the immunofluorescence results showed that the number of punctate fluorescent autophagosomes induced in the LPS + NaHS group was significantly reduced in the LPS + NaHS + 3-MA group (Fig. 4D and E). These results demonstrated that 3-MA effectively inhibited the level of autophagy. Next, the effects of 3-MA on HK-2 cell apoptosis and the release of inflammatory factors were examined. The apoptosis rate of HK-2 cells and the levels of released IL-1β and IL-18 were significantly increased in the LPS + NaHS + 3-MA group compared with the LPS + NaHS group (Fig. 4F-I), indicating that the autophagy block by 3-MA partially reversed the protective effect of NaHS on LPS-induced apoptosis and the release of inflammatory factors in HK-2 cell.

Inhibition of autophagy by 3-MA reverses the protective effect of NaHS on LPS-induced AKI in mice. To further verify the aforementioned protective effect of NaHS in animals, 3-MA was intraperitoneally injected into mice to inhibit autophagy and it was examined whether the protective effect of NaHS still existed in mice. As shown in Fig. 5, western blotting and immunofluorescence results on mouse kidney tissue showed that the ratio of LC3B-II/LC3B-I was significantly reduced in the LPS + NaHS + 3-MA group, and the expression of p62 protein was increased compared with the LPS + NaHS group (Fig. 5A-C). Furthermore, the immunofluorescence results showed that the number of punctate fluorescent autophagosomes induced in the LPS + NaHS group was notably reduced in the LPS + NaHS + 3-MA group (Fig. 5D). Thus, these results suggested that 3-MA effectively blocked the autophagy induced by NaHS. Based on these findings, the renal function, kidney morphological changes, release of inflammatory factors and level of apoptosis were examined in mice. Compared with the LPS + NaHS group, the BUN and creatinine levels in the LPS + NaHS + 3-MA group were significantly increased (Fig. 5E and F). H&E staining showed that the tissue structure damage, such as edema of tubular epithelial cells, in the LPS + NaHS + 3-MA group was aggravated (Fig. 5G and H). Consistently, ELISA results showed that the release of IL-1β and IL-18 in serum and kidney tissues was significantly higher in the LPS + NaHS + 3-MA group than that in the LPS + NaHS group (Fig. 5I-L). TUNEL staining also showed that the apoptosis rate of renal tubular cells in the LPS + NaHS + 3-MA group was significantly higher than that in the LPS + NaHS group (Fig. 5M and N).

Discussion

The pathogenesis of AKI is very complicated, it involves hemodynamic changes, apoptosis, inflammation, coagulation activation and oxidative stress (5). Renal tubular epithelial cells are the main target cell type of AKI. In the environment with ischemia and/or toxins, renal tubular epithelial cells undergo
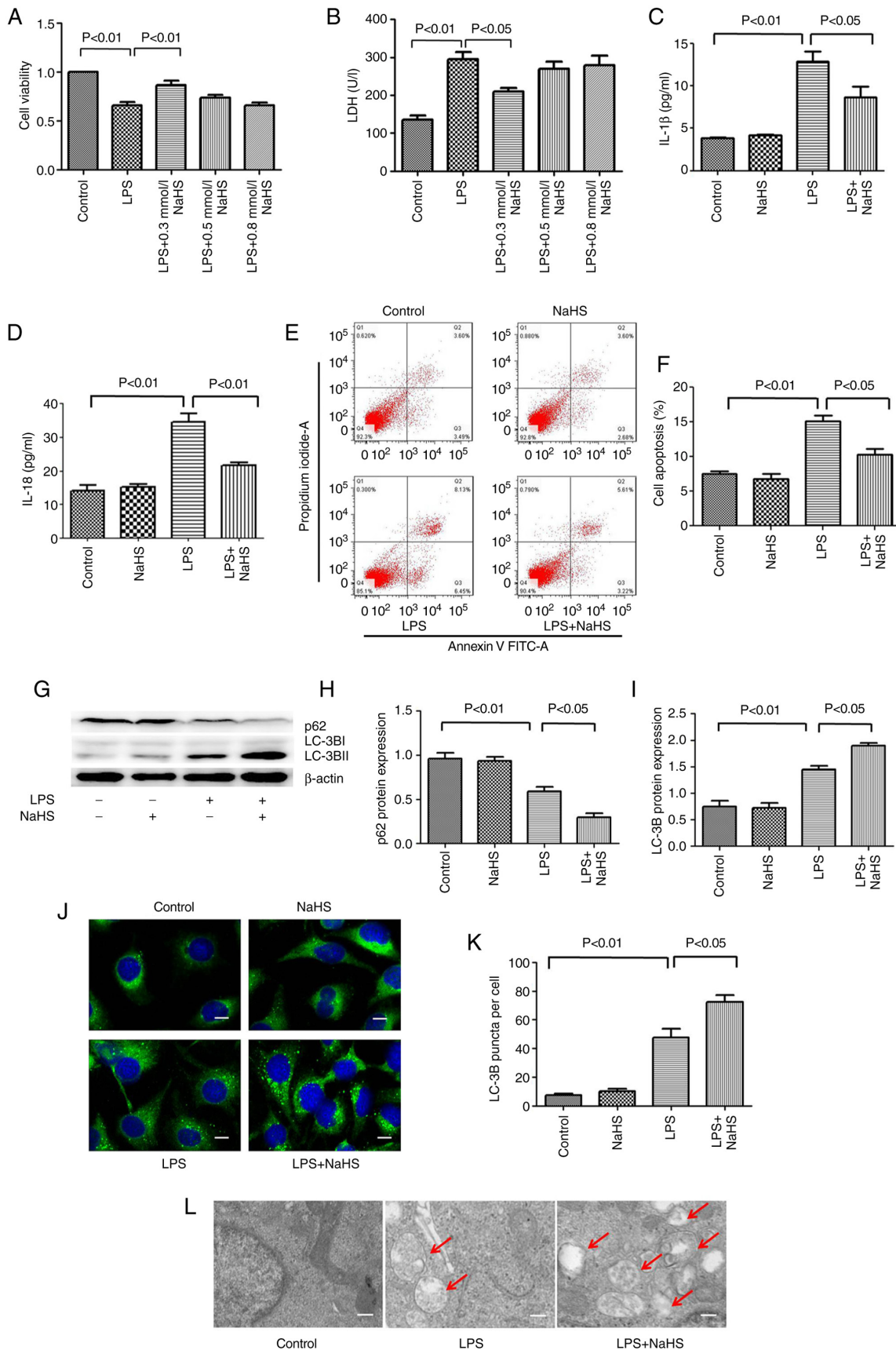
Figure 3. Hydrogen sulfide reduces the release of inflammatory factors and apoptosis in HK-2 cells induced by LPS, and promotes autophagy. (A) Cell viability detected by Cell Counting Kit-8 assay. (B) LDH release level. (C) IL-1β and (D) IL-18 levels in cell supernatant. (E) The percentage of apoptotic cells in each group detected by flow cytometry. (F) Statistics of apoptosis index. (G) Expression levels of LC3B and p62 proteins. (H) The ratio of p62/β-actin. (I) The ratio of LC3B-II/LC3B-I. (J) Immunofluorescence analysis of LC3B punctate aggregation in cells. Scale bar, 20 μm. (K) Statistics of the average number of autophagosomes in each group. (L) The autophagy level in kidney tissue under transmission electron microscope. Scale bar, 2 mm. The red arrows indicate autophagosome. Data are presented as the mean ± SD and represent three independent experiments. LPS, lipopolysaccharide; LDH, lactic dehydrogenase; IL, interleukin; LC3B, microtubule associated protein 1 light chain 3; NaHS, sodium hydrosulfide hydrate.
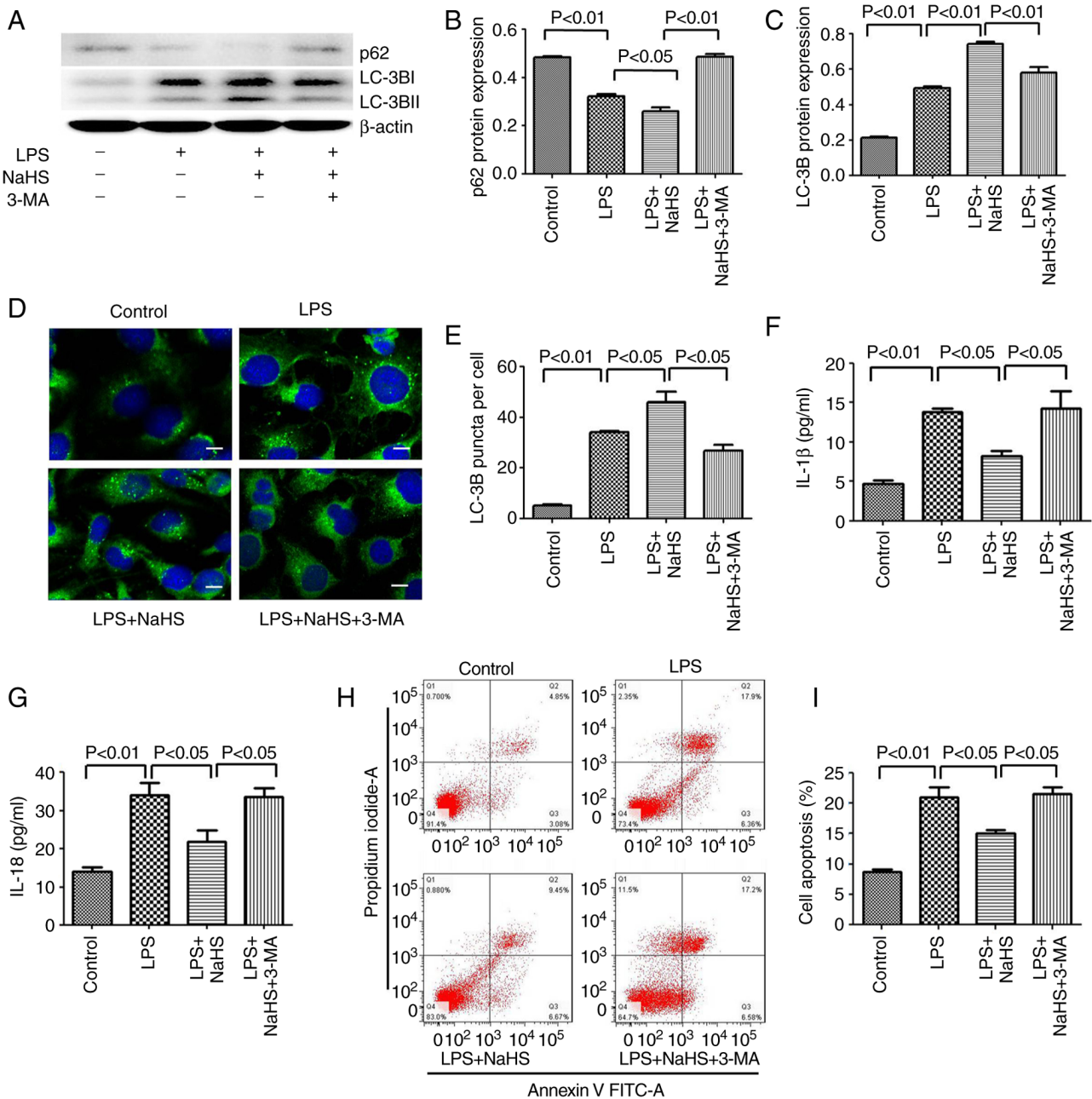
Figure 4. 3-MA reverses the anti-inflammatory and anti-apoptotic effects of hydrogen sulfide on HK-2 cells by inhibiting autophagy. (A) The expression of LC3B and p62 proteins in HK-2 cells after 3-MA treatment. (B) The ratio of p62/β-actin. (C) The ratio of LC3B-II/LC3B-I. (D) Immunofluorescence analysis of LC3B punctate aggregation in cells. Scale bar, 20 μm. (E) Statistics of the average number of autophagosomes in each group. (F) Level of IL-1β in cell supernatant after 3-MA treatment. (G) Level of IL-18 in cell supernatant after 3-MA treatment. (H) The apoptosis rate detected by flow cytometry after 3-MA treatment. (I) Statistics of apoptosis index. Data are presented as the mean ± SD and represent three independent experiments. 3-MA, 3-methyladenine; LC3B, microtubule associated protein 1 light chain 3; IL, interleukin; NaHS, sodium hydrosulfide hydrate; LPS, lipopolysaccharide.

necrosis, apoptosis and shedding, which is an important cause of AKI (31). In addition, the inflammatory response of kidney is also an important factor involved in the occurrence and development of AKI (31). It is known that LPS and other pathogen-related molecular patterns (PAMP) can directly interact with toll-like receptor (TLR)-2 and TLR-4 on renal tubular epithelial cells (TEC), and induce the release of IL-6, TNF-α and other cytokines (32-34). This pro-inflammatory effect on TEC eventually leads to infiltration of white blood cells, which promotes tissue damage (5). In the present study, LPS was used to construct septic a AKI mouse model and cell injury model. The kidney tissue and cells showed obvious

damage, and the apoptosis rate and the release of inflammatory factors were significantly increased.

As a gas signal molecule, H₂S plays an important role in the human body. 1/3 of H₂S exists as gas molecules in the body and 2/3 is in the form of NaHS, which not only ensures the stability of H₂S in the body, but also does not change the pH level of the internal environment (35). Thus, the current study chose NaHS as the H₂S donor. Studies shows that different concentrations of H₂S have different effects, such as low concentrations have protection (12,36), and high concentrations have damaging effects (37,38). Therefore, our study choose a low concentration dose. In the future, we will
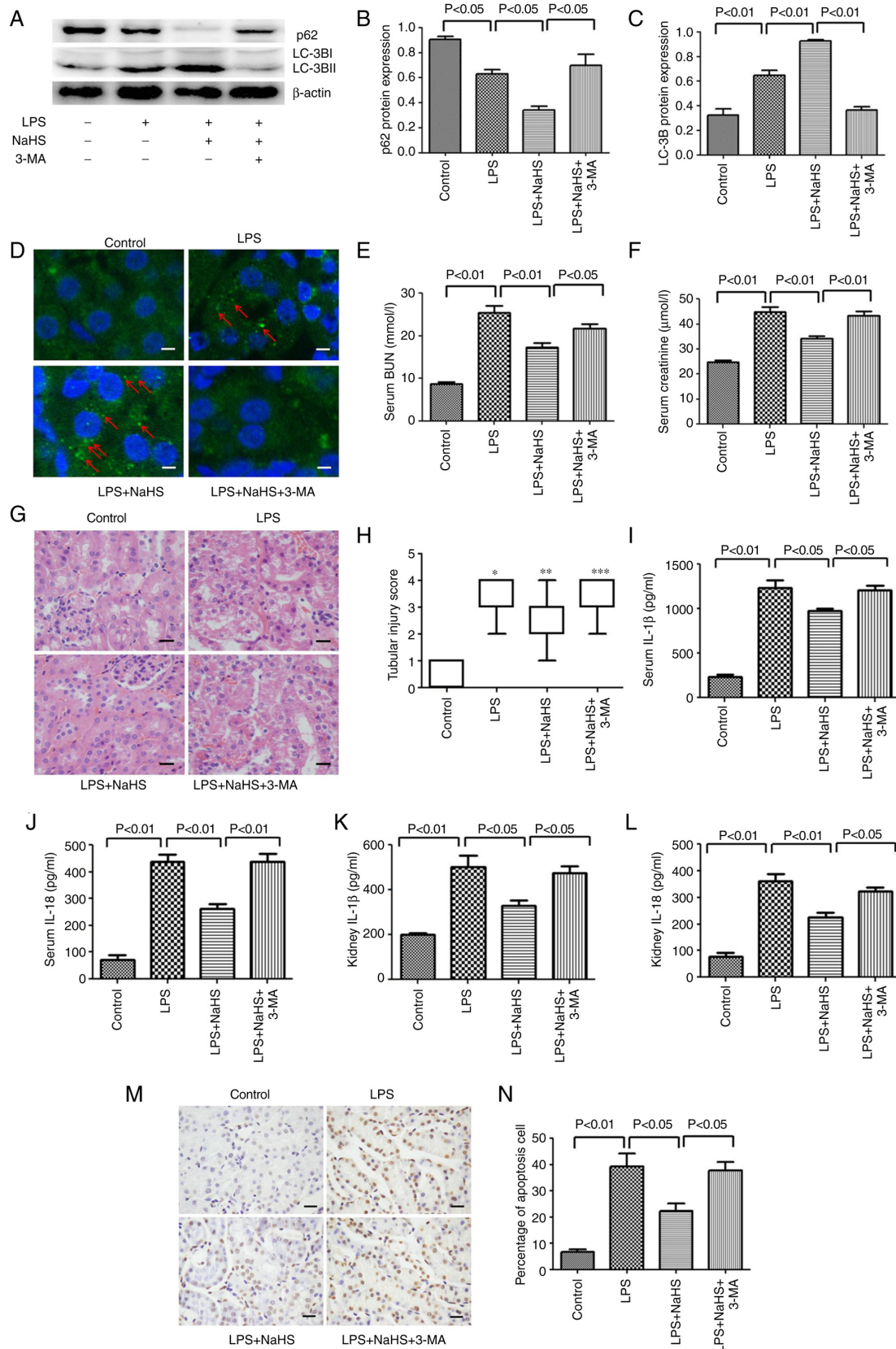
Figure 5. 3-MA reverses the protective effect of hydrogen sulfide on LPS-induced acute kidney injury in mice by inhibiting autophagy. (A) The expression of LC3B and p62 proteins in mouse kidney tissues after 3-MA treatment. (B) The ratio of p62/β-actin. (C) The ratio of LC3B-II/LC3B-I. (D) Immunofluorescence analysis of LC3B punctate aggregation in kidney tissue. Scale bar, 20 μm. The red arrows indicate autophagosome. (E) The BUN level in mouse serum after 3-MA treatment. (F) The creatine level in mouse serum after 3-MA treatment. (G) The morphological changes of kidney tissue under light microscope after 3-MA treatment (hematoxylin and eosin staining). Scale bar, 20 μm. (H) Histological damage score of mouse kidney. *P<0.01 vs. control group; **P<0.01 vs. LPS group; ***P<0.01 vs. LPS + NaHS group. (I) IL-1β and (J) IL-18 levels in mouse serum after 3-MA treatment. (K) IL-1β and (L) IL-18 levels in kidney tissue after 3-MA treatment. (M) TUNEL staining shows the level of apoptosis in kidney tissue after 3-MA treatment. Scale bar, 20 μm. (N) Statistics of apoptosis index in mouse kidney tissue of each group. Data are presented as the mean ± SD (n=10). 3-MA, 3-methyladenine; LPS, lipopolysaccharide; LC3B, microtubule associated protein 1 light chain 3; IL, interleukin; BUN, blood urea nitrogen; NaHS, sodium hydrosulfide hydrate.

verify the optimal dosage of H_2S in follow-up experiments. The protective mechanisms of H_2S include anti-inflammatory and antioxidant effects, and regulation of cell proliferation and apoptosis (12-18,39). The present results also showed that NaHS can reduce LPS-induced kidney damage through anti-inflammatory and anti-apoptotic effects. The anti-inflammatory and anti-apoptotic mechanism of NaHS is still unclear. In previous years, studies have shown that H_2S also has a regulatory effect on autophagy. For example, H_2S can promote liver autophagy, reduce serum triglyceride levels and improve non-alcoholic fatty liver disease (40). Yang *et al* (26) found that H_2S can prevent diabetic cardiomyopathy by activating autophagy. The present study also found that pretreatment with NaHS further promoted the level of autophagy in HK-2 cells stimulated by LPS, suggesting that the protective effect of NaHS may be through regulating autophagy.

So far, a large number of studies have shown that autophagy has a regulatory effect on apoptosis and the release of inflammatory factors. For example, in cisplatin-induced renal tubular cell injury, both autophagy and caspases are activated, and the activation of autophagy is earlier than the activation of caspases (41-43). In renal tubular epithelial cells cultured *in vitro*, inhibition of cisplatin-induced autophagy by 3-MA and knockdown of autophagy gene Atg5 or Beclin1 via siRNA can enhance the activation of caspase-3, 7, 6 (41,43) and apoptosis (41-43); and overexpression of Atg5 and Beclin-1 protein can prevent the cisplatin-induced activation of caspase and apoptosis (44). The specific knockout of Atg5 or Atg7 in mouse proximal tubular cells has been found to inhibit autophagy and enhance cisplatin-induced apoptosis and caspase activity (23,44). In addition, Han *et al* (46) showed that the autophagy induced by AXL receptor tyrosine kinase could reduce acute liver injury by inhibiting the activation of NLRP3 inflammasome. Tong *et al* (47) found that heat shock factor 1 could inhibit the release of inflammatory factors by inducing autophagy, thus exerting a protective effect on septic mice. Since the activation of autophagy can inhibit apoptosis and the release of inflammatory factors, the protective effect of NaHS observed in this study could also be mediated by regulating autophagy. To test this hypothesis, the autophagy inhibitor 3-MA was used to block autophagy both *in vivo* and *in vitro*. The results showed that 3-MA pretreatment significantly inhibited the protective effect of NaHS, suggesting that NaHS inhibited renal tubular cell apoptosis and renal interstitial inflammation by promoting autophagy, thereby protecting from the AKI induced by LPS. The aforementioned results indicated that the regulation of autophagy by NaHS may be a key protective mechanism to alleviate AKI. Recently, studies have reported that H_2S can activate autophagy by inhibiting the MAPK pathway, thereby exerting anti-inflammatory and anti-apoptotic effects (48,49). H_2S can also induce autophagy by activating AMPK (26,50). In addition, H_2S can induce autophagy by activating the Nrf2/Keap1 signaling pathway and play a protective role (51-53). However, how NaHS regulates autophagy in LPS-induced AKI is not yet fully elucidated and further investigation is needed.

In summary, this study found that NaHS can prevent AKI in mice with endotoxemia, and its protective effect is partially mediated by promoting autophagy to inhibit renal tubular epithelial cell apoptosis and the release of inflammatory factors.

Availability of data and materials

The datasets used and/or analyzed during the current study are available from the corresponding author on reasonable request.

Authors' contributions

TL, JZ and YL conceived and designed the experiments. TL, JZ, SM and YC performed the experiments and analyzed the samples. TL and YX analyzed the data. TL wrote the manuscript. All authors interpreted the data and critically revised the manuscript for important intellectual contents. All authors have read and approved the final manuscript. TL and YL confirm the authenticity of all the raw data.

Ethics approval and consent to participate

All animal experiments were approved by the Institutional Animal Ethics Committee of Central South University (Changsha, China).

Patient consent for publication

Not applicable.

Competing interests

The authors declare that they have no competing interests.

References

1. Alberti C, Brun-Buisson C, Burchardi H, Martin C, Goodman S, Artigas A, Sicignano A, Palazzo M, Moreno R, Boulmé R, *et al*: Epidemiology of sepsis and infection in ICU patients from an international multicentre cohort study. Intensive Care Med 28: 108-121, 2002.
2. Hotchkiss RS and Karl IE: The pathophysiology and treatment of sepsis. N Engl J Med 348: 138-50, 2003.
3. Bagshaw SM, George C and Bellomo R; ANZICS Database Management Committee: Early acute kidney injury and sepsis: A multicentre evaluation. Crit Care 12: R47, 2008.
4. Mehta RL, Bouchard J, Soroko SB, Ikizler TA, Paganini EP, Chertow GM and Himmelfarb J; Program to Improve Care in Acute Renal Disease (PICARD) Study Group: Sepsis as a cause and consequence of acute kidney injury: Program to improve care in Acute Renal Disease. Intensive Care Med 37: 241-248, 2011.

5. Gomez H, Ince C, De Backer D, Pickkers P, Payen D, Hotchkiss J and Kellum JA: A unified theory of sepsis-induced acute kidney injury: Inflammation, microcirculatory dysfunction, bioenergetics, and the tubular cell adaptation to injury. Shock 41: 3-11, 2014.
6. Peerapornratana S, Manrique-Caballero CL, Gómez H and Kellum JA: Acute kidney injury from sepsis: Current concepts, epidemiology, pathophysiology, prevention and treatment. Kidney Int 96: 1083-1099, 2019.
7. Szabo C: Hydrogen sulphide and its therapeutic potential. Nat Rev Drug Discov 6: 917-935, 2007.
8. Ahangarpour A, Abdollahzade Fard A, Gharibnaseri MK, Jalali T and Rashidi I: Hydrogen sulfide ameliorates the kidney dysfunction and damage in cisplatin-induced nephrotoxicity in rat. Vet Res Forum 5: 121-127, 2014.
9. Bos EM, Leuvenink HG, Snijder PM, Kloosterhuis NJ, Hillebrands JL, Leemans JC, Florquin S and van Goor H: Hydrogen sulfide-induced hypometabolism prevents renal ischemia/reperfusion injury. J Am Soc Nephrol 20: 1901-1905, 2009.
10. Han SJ, Kim JI, Park JW and Park KM: Hydrogen sulfide accelerates the recovery of kidney tubules after renal ischemia/reperfusion injury. Nephrol Dial Transplant 30: 1497-1506, 2015.
11. Zhu JX, Kalbfleisch M, Yang YX, Bihari R, Lobb I, Davison M, Mok A, Cepinskas G, Lawendy AR and Sener A: Detrimental effects of prolonged warm renal ischaemia-reperfusion injury are abrogated by supplemental hydrogen sulphide: An analysis using real-time intravital microscopy and polymerase chain reaction. BJU Int 110: E1218-E1227, 2012.
12. Zhou X, Feng Y, Zhan Z and Chen J: Hydrogen sulfide alleviates diabetic nephropathy in a streptozotocin-induced diabetic rat model. J Biol Chem 289: 28827-28834, 2014.
13. Lee HJ, Mariappan MM, Feliers D, Cavaglieri RC, Sataranatarajan K, Abboud HE, Choudhury GG and Kasinath BS: Hydrogen sulfide inhibits high glucose-induced matrix protein synthesis by activating AMP-activated protein kinase in renal epithelial cells. J Biol Chem 287: 4451-4461, 2012.
14. Safar MM and Abdelsalam RM: H2S donors attenuate diabetic nephropathy in rats: Modulation of oxidant status and polyol pathway. Pharmacol Rep 67: 17-23, 2015.
15. Jiang D, Zhang Y, Yang M, Wang S, Jiang Z and Li Z: Exogenous hydrogen sulfide prevents kidney damage following unilateral ureteral obstruction. Neurourol Urodyn 33: 538-543, 2014.
16. Song K, Wang F, Li Q, Shi YB, Zheng HF, Peng H, Shen HY, Liu CF and Hu LF: Hydrogen sulfide inhibits the renal fibrosis of obstructive nephropathy. Kidney Int 85: 1318-1329, 2014.
17. Dursun M, Otunctemur A, Ozbek E, Sahin S, Besiroglu H, Ozsoy OD, Cekmen M, Somay A and Ozbay N: Protective effect of hydrogen sulfide on renal injury in the experimental unilateral ureteral obstruction. Int Braz J Urol 41: 1185-1193, 2015.
18. Chen Y, Jin S, Teng X, Hu Z, Zhang Z, Qiu X, Tian D and Wu Y: Hydrogen sulfide attenuates LPS-Induced acute kidney injury by inhibiting inflammation and oxidative stress. Oxid Med Cell Longev 2018: 6717212, 2018.
19. Levine B and Klionsky DJ: Development by self-digestion: Molecular mechanisms and biological functions of autophagy. Dev Cell 6: 463-477, 2004.
20. Mizushima N, Yoshimori T and Ohsumi Y: The role of Atg proteins in autophagosome formation. Annu Rev Cell Dev Biol 27: 107-132, 2011.
21. Hsiao HW, Tsai KL, Wang LF, Chen YH, Chiang PC, Chuang SM and Hsu C: The decline of autophagy contributes to proximal tubular dysfunction during sepsis. Shock 37: 289-296, 2012.
22. Leventhal JS, Ni J, Osmond M, Lee K, Gusella GL, Salem F and Ross MJ: Autophagy limits endotoxemic acute kidney injury and alters renal tubular epithelial cell cytokine expression. PLoS One 11: e150001, 2016.
23. Jiang M, Wei Q, Dong G, Komatsu M, Su Y and Dong Z: Autophagy in proximal tubules protects against acute kidney injury. Kidney Int 82: 1271-1283, 2012.
24. Liu S, Hartleben B, Kretz O, Wiech T, Igarashi P, Mizushima N, Walz G and Huber TB: Autophagy plays a critical role in kidney tubule maintenance, aging and ischemia-reperfusion injury. Autophagy 8: 826-837, 2012.
25. Li T, Liu Y, Zhao J, Miao S, Xu Y, Liu K, Liu M, Wang G and Xiao X: Aggravation of acute kidney injury by mPGES-2 down regulation is associated with autophagy inhibition and enhanced apoptosis. Sci Rep 7: 10247, 2017.
26. Yang F, Zhang L, Gao Z, Sun X, Yu M, Dong S, Wu J, Zhao Y, Xu C, Zhang W and Lu F: Exogenous H2S protects against diabetic cardiomyopathy by activating autophagy via the AMPK/mTOR Pathway. Cell Physiol Biochem 43: 1168-1187, 2017.
27. Liu Y, Liao R, Qiang Z, Yang W, Cao J and Zeng H: Exogenous H2S protects colon cells in ulcerative colitis by inhibiting NLRP3 and activating autophagy. DNA Cell Biol 40: 748-756, 2021.
28. Zhang S, Yang G, Guan W, Li B, Feng X and Fan H: Autophagy plays a protective role in sodium hydrosulfide-induced acute lung injury by attenuating oxidative stress and inflammation in rats. Chem Res Toxicol 34: 857-864, 2021.
29. Zhao Y, Feng X, Li B, Sha J, Wang C, Yang T, Cui H and Fan H: Dexmedetomidine protects against lipopolysaccharide-induced acute kidney injury by enhancing autophagy through inhibition of the PI3K/AKT/mTOR pathway. Front Pharmacol 11: 128, 2020.
30. Hu L, Guo J, Zhou L, Zhu S, Wang C, Liu J, Hu S, Yang M and Lin C: Hydrogen sulfide protects retinal pigment epithelial cells from oxidative stress-induced apoptosis and affects autophagy. Oxid Med Cell Longev 2020: 8868564, 2020.
31. Lerolle N, Nochy D, Guérot E, Bruneval P, Fagon JY, Diehl JL and Hill G: Histopathology of septic shock induced acute kidney injury: Apoptosis and leukocytic infiltration. Intensive Care Med 36: 471-478, 2010.
32. Zhang B, Ramesh G, Uematsu S, Akira S and Reeves WB: TLR4 signaling mediates inflammation and tissue injury in nephrotoxicity. J Am Soc Nephrol 19: 923-932, 2008.
33. Ho AW, Wong CK and Lam CW: Tumor necrosis factor-alpha up-regulates the expression of CCL2 and adhesion molecules of human proximal tubular epithelial cells through MAPK signaling pathways. Immunobiology 213: 533-544, 2008.
34. Allam R, Scherbaum CR, Darisipudi MN, Mulay SR, Hägele H, Lichtnekert J, Hagemann JH, Rupanagudi KV, Ryu M, Schwarzenberger C, et al: Histones from dying renal cells aggravate kidney injury via TLR2 and TLR4. J Am Soc Nephrol 23: 1375-1388, 2012.
35. Hosoki R, Matsuki N and Kimura H: The possible role of hydrogen sulfide as an endogenous smooth muscle relaxant in synergy with nitric oxide. Biochem Biophys Res Commun 237: 527-531, 1997.
36. Lin F, Liao C, Sun Y, Zhang J, Lu W, Bai Y, Liao Y, Li M, Ni X, Hou Y, et al: Hydrogen sulfide inhibits cigarette smoke-induced endoplasmic reticulum stress and apoptosis in bronchial epithelial cells. Front Pharmacol 8: 675, 2017.
37. Feng X, Zhang H, Shi M, Chen Y, Yang T and Fan H: Toxic effects of hydrogen sulfide donor NaHS induced liver apoptosis is regulated by complex IV subunits and reactive oxygen species generation in rats. Environ Toxicol 35: 322-332, 2020.
38. Ahmad A, Druzhyna N and Szabo C: Delayed treatment with sodium hydrosulfide improves regional blood flow and alleviates cecal ligation and puncture (CLP)-Induced septic shock. Shock 46: 183-193, 2016.
39. Chen YH, Teng X, Hu ZJ, Tain DY, Jin S and Wu YM: Hydrogen sulfide attenuated sepsis-induced myocardial dysfunction through TLR4 pathway and endoplasmic reticulum stress. Front Physiol 12: 653601, 2021.
40. Sun L, Zhang S, Yu C, Pan Z, Liu Y, Zhao J, Wang X, Yun F, Zhao H, Yan S, et al: Hydrogen sulfide reduces serum triglyceride by activating liver autophagy via the AMPK-mTOR pathway. Am J Physiol Endocrinol Metab 309: E925-E935, 2015.
41. Yang C, Kaushal V, Shah SV and Kaushal GP: Autophagy is associated with apoptosis in cisplatin injury to renal tubular epithelial cells. Am J Physiol Renal Physiol 294: F777-F787, 2008.
42. Periyasamy-Thandavan S, Jiang M, Wei Q, Smith R, Yin XM and Dong Z: Autophagy is cytoprotective during cisplatin injury of renal proximal tubular cells. Kidney Int 74: 631-640, 2008.
43. Kaushal GP, Kaushal V, Herzog C and Yang C: Autophagy delays apoptosis in renal tubular epithelial cells in cisplatin cytotoxicity. Autophagy 4: 710-712, 2008.
44. Herzog C, Yang C, Holmes A and Kaushal GP: zVAD-fmk prevents cisplatin-induced cleavage of autophagy proteins but impairs autophagic flux and worsens renal function. Am J Physiol Renal Physiol 303: F1239-F1250, 2012.
45. Yang Z and Klionsky DJ: Mammalian autophagy: Core molecular machinery and signaling regulation. Curr Opin Cell Biol 22: 124-131, 2010.
46. Han J, Bae J, Choi CY, Choi SP, Kang HS, Jo EK, Park J, Lee YS, Moon HS, Park CG, et al: Autophagy induced by AXL receptor tyrosine kinase alleviates acute liver injury via inhibition of NLRP3 inflammasome activation in mice. Autophagy 12: 2326-2343, 2016.
47. Tong Z, Jiang B, Zhang L, Liu Y, Gao M, Jiang Y, Li Y, Lu Q, Yao Y and Xiao X: HSF-1 is involved in attenuating the release of inflammatory cytokines induced by LPS through regulating autophagy. Shock 41: 449-453, 2014.

48. Zhang GY, Lu D, Duan SF, Gao YR, Liu SY, Hong Y, Dong PZ, Chen YG, Li T, Wang DY, *et al*: Hydrogen sulfide alleviates lipopolysaccharide-induced diaphragm dysfunction in rats by reducing apoptosis and inflammation through ROS/MAPK and TLR4/NF-κB signaling pathways. Oxid Med Cell Longev 2018: 9647809, 2018.

49. Han X, Mao Z, Wang S, Xin Y, Li P, Maharjan S and Zhang B: GYY4137 protects against MCAO via p38 MAPK mediated anti-apoptotic signaling pathways in rats. Brain Res Bull 158: 59-65, 2020.

50. Wang H, Zhong P and Sun L: Exogenous hydrogen sulfide mitigates NLRP3 inflammasome-mediated inflammation through promoting autophagy via the AMPK-mTOR pathway. Biol Open 8: bio043653, 2019.

51. Zhao S, Song T, Gu Y, Zhang Y, Cao S, Miao Q, Zhang X, Chen H, Gao Y, Zhang L, *et al*: Hydrogen sulfide alleviates liver injury Through the S-Sulfhydrated-Kelch-Like ECH-Associated Protein 1/Nuclear Erythroid 2-Related Factor 2/Low-Density Lipoprotein Receptor-Related Protein 1 pathway. Hepatology 73: 282-302, 2021.

52. Wu J, Tian Z, Sun Y, Lu C, Liu N, Gao Z, Zhang L, Dong S, Yang F, Zhong X, *et al*: Exogenous H₂S facilitating ubiquitin aggregates clearance via autophagy attenuates type 2 diabetes-induced cardiomyopathy. Cell Death Dis 8: e2992, 2017.

53. Zhao S, Yang L, Li L and Fan Z: NaHS alleviated cell apoptosis and mitochondrial dysfunction in remote lung tissue after renal ischemia and reperfusion via Nrf2 activation-mediated NLRP3 pathway inhibition. Biomed Res Int 2021: 5598869, 2021.